6-3-2009

The Relationship between Liver Fat Content and Unenhanced Computed Tomography

Karen Shoebotham

The Relationship between Liver Fat Content and Unenhanced Computed Tomography

A Thesis Submitted to the
Yale University School of Medicine
in Partial Fulfillment of the Requirement
for the Degree of Doctor of Medicine

By
Karen Shoebotham
2008

THE RELATIONSHIP BETWEEN LIVER FAT CONTENT AND UNENHANCED COMPUTED TOMOGRAPHY.

Karen Shoebotham and Kinh Gian Do. Department of Radiology, NYU School of Medicine, New York, NY. (Sponsored by Jeffrey C. Weinreb, Department of Diagnostic Radiology, Yale University School of Medicine).

The purpose of this study was to chart unenhanced CT liver and spleen attenuation data on patients with normal and fatty livers to demonstrate a relationship between liver fat content and attenuation on unenhanced CT using MR chemical shift imaging as a reference standard. Retrospective data was gathered on 116 patients from NYU Tisch Hospital who had undergone both an unenhanced CT and MR opposed-phase imaging of the liver within 2 months. MR fat fraction (MR FF) was calculated using signal decrease on in-phase and opposed-phase imaging, with a cutoff of 0.2 considered significant fatty infiltration. Three CT liver attenuation indices were obtained: liver attenuation, liver minus spleen attenuation, and liver to spleen ratio. For each index, linear regression was performed and 95% confidence intervals calculated. Receiver operating characteristic (ROC) analyses were performed to determine the accuracy and optimal cutoff values for the best balance between sensitivity and specificity, and the highest cutoff value that had 100% specificity was determined. ROC analysis showed good accuracy of all CT indices, with sensitivities and specificities between 91 and 93% for cutoff values of 50, 0, and 1.0 for CT liver attenuation, liver minus spleen, and liver to spleen ratio, respectively. Correlation of hepatic steatosis between unenhanced CT and MR opposed-phase imaging was excellent, but as MR imaging is not the gold standard for determining liver fat content, conclusions drawn from this study depend on the accuracy of MR imaging as determined in other studies.

Acknowledgements

I would like to thank Dr. Jeffrey Weinreb for agreeing to act as my advisor in my thesis project; he has shown exceptional patience as I made halting progress toward completion of this project. And certainly, thanks to Dolores Depalma, who always knew were Dr. Weinreb was, and often provided some refreshments in the meantime. I appreciate the rapid and helpful responses of Dr. Kevin Johnson in listening to my project idea then bearing with me when the topic of my project had to be changed. Dr. Lawrence Staib was indispensible in both doing the statistical calculations and providing graphics of those results. The entire department of radiology here at Yale New Haven Hospital has been encouraging and wonderful to work with over the past two years.

Thanks to Richard Do, who came up with the project, did preliminary data collection, and returned to the raw data to clarify details of scanners and parameters used in the imaging; by extension, I must thank Dr. John Bonavita and the NYU department of radiology where all data were obtained.

I can also thank my father for his encouragement and for the care package, containing all necessary junk food and caffeinated beverages.

Finally, thanks to Greg Salmieri, who at this moment is working on approximately the five-hundredth page of his dissertation, for listening to me while I procrastinated and moaned, providing a lot of much needed perspective.

Table of Contents

Introduction

Hepatic Steatosis

Hepatic steatosis, or fatty liver, is an accumulation of vesicles of fats, primarily triglycerides, within hepatocytes, generally considered abnormal when greater than 5 to 10 percent of the liver volume. Hepatic steatosis is the early manifestation of a spectrum of liver damage which may progress to steatohepatitis and, eventually, cirrhosis. It can exist as either a temporary or chronic state. Hepatic steatosis is characterized by a lack of inflammation, cell death, or scarring and, importantly, is considered reversible. Estimates of the prevalence of hepatic steatosis are difficult to make because it is typically asymptomatic, and a significant number of cases are undiagnosed. However, based on cross-sectional and autopsy studies, it is estimated to affect between 10 and 35 percent of the general population (1, 2, 3). Prevalence varies considerably by the population being studied with ethnicity and rates of alcoholism, obesity and insulin resistance playing major roles (1, 4).

Once considered a benign condition, hepatic steatosis has gained increased attention in recent years both because of its association with obesity and metabolic syndrome, as well as greater awareness of the potential to progress to steatohepatitis and cirrhosis, with an attendant increase in the risk for hepatocellular carcinoma. In

addition to these concerns, the importance of a significant percentage of fatty infiltration in liver transplant, including those involving living donor liver transplant, to outcomes of both donor and recipient, has fueled interest in the non-invasive diagnosis and treatment of hepatic steatosis (5).

Causes of Hepatic Steatosis

Fatty liver can occur because of excess importation of free fatty acids from adipose tissue, from decreased hepatic export of fatty acids (secondary to reduced synthesis or secretion of VLDL), from impaired beta-oxidation of free fatty acids, or from some combination of these (6). Fatty liver disease is typically classified according to its cause, with the primary distinction being whether or not it is related to alcohol-induced hepatic damage. Alcoholic liver disease (ALD) and nonalcoholic fatty liver disease (NAFLD) have essentially identical histopathologic manifestations, and cannot be differentiated by biopsy (4). NAFLD can currently be diagnosed only in patients with liver disease in whom a history of significant alcohol intake has been exhaustively ruled out. Among the causes of NAFLD are drugs such as corticosteroids, certain chemotherapeutic agents, total parental nutrition, rapid weight loss, or diseases affecting lipid metabolism such as lipodystrophy (2). However, the great majority of cases of NAFLD are associated with one or more components of metabolic syndrome such as obesity and insulin resistance.

Treatment

As mentioned above, hepatic steatosis, unlike later stages of liver disease such as cirrhosis, is at least theoretically completely reversible, with treatment consisting of the removal of its cause. In the case of alcoholic liver disease, cessation of alcohol is of primary importance. The vast majority of cases of NAFLD are associated with obesity, and the American Gastroenterological Association recommends weight loss for patients diagnosed with NAFLD (7). Some small studies demonstrate improvements in liver enzymes and decreases in steatosis on biopsy following weight loss surgery (8, 9). This is, however, to be reconciled with data that indicate that very rapid weight loss, such as that which may follow weight loss surgery, often increases hepatic steatosis, especially in patients who already have NAFLD (10).

Betaine, a drug used to treat homocystinuria, has been used in small trials in patients with NASH, and in one study in which it was combined with other supplements, a 25% reduction in hepatic steatosis was seen after eight weeks (11). Some studies have shown improvement in hepatic steatosis in patients with non-alcoholic steatohepatitis (NASH) after metformin therapy (12) or treatment with pioglitazone (13). However, large trials validating the role of any pharmacologic agent for reduction of hepatic steatosis in humans are lacking. Other common treatments for obesity, dyslipidemia, and insulin resistance such as exercise, lipid lowering agents, and antioxidants as yet have little evidence in humans of efficacy on liver fat as measured by histology, but are generally recommended, given the strong correlation between obesity and NAFLD (4).

Role of Hepatic Steatosis in Liver Surgery

One aspect of hepatic steatosis of particular interest is its role in transplant surgery. Specifically, a high percentage of fatty infiltration in the liver is associated with poor post-surgical outcomes for both living liver donors and transplant recipients. Specifically, macrosteatosis above 30% is associated with higher rates of initial graft non-function, elevated liver enzymes following surgery, and graft failure (14, 15). Two patterns of hepatic steatosis, macrovesicular and microvesicular, are generally differentiated. Macrovesicular steatosis is defined as a single, large vacuole in a given hepatocyte, larger than the nucleus, while microvesicular steatosis is characterized by multiple small vacuoles within a hepatocyte; many patients have a mixed pattern of micro and macrovesicular steatosis. Some controversy exists concerning the relative importance of these two patterns in contributing to short and long-term complications following liver transplantation. In particular, microvesicular steatosis is not well visualized with the conventional hematoxylin and eosin staining used in screening for hepatic steatosis, which may lead to its prevalence being underestimated (16). However, microvesicular fat appears to have less of a negative impact on outcomes after transplantation, and levels of microsteatosis above 30% may not preclude safe transplantation (17).

Another perspective on surgical risk concerns the risk to healthy living liver donors, for whom risk considerations are different than those of potential transplant recipients. Patients awaiting transplant are typically already very ill; the trade-off of earlier transplantation with a suboptimal specimen must be weight against continued

decline in health and, indeed, ability to benefit from transplantation at all if it is delayed. Function of residual liver tissue following partial hepatectomy is also of concern when this surgery is performed to remove tumors, including hepatocellular carcinoma and metastatic disease. Aside from the prevalence of NAFLD in the general population, which appears similar in liver donors (15, 17), patients undergoing chemotherapeutic treatment prior to partial hepatectomy may develop or increase their level of hepatic steatosis, and steatosis in this patient group is an independent risk factor for complications following resection (18). In some studies, chemotherapy appears to increase risk of post-operative morbidity regardless of the agent used, instead correlating with the number of cycles of chemotherapy (19), but particular agents such as 5-flurouracil, oxaliplatin and especially irinotecan appear to increase the risk of developing hepatic steatosis and may even lead to chemotherapy-associated steatohepatitis (CASH). CASH is strongly associated with increased postoperative morbidity and mortality (20, 21). Despite these risks, it is not agreed whether patients should undergo biopsy prior to resection to screen for steatosis and CASH (21, 22).

Diagnosis

Hepatic steatosis is often first suspected when blood tests reveal elevated levels of liver transaminases. Indeed, NAFLD is the most common cause of abnormal liver enzymes in adults without a known cause of liver disease, and may in fact be the most common overall cause of elevated liver enzymes in American adults (4, 23). However, liver enzyme values are within normal limits for up to 78% of patients with NAFLD, and

even disease which is histologically advanced may not lead to elevated liver enzymes, and cannot be ruled out with this method (1). Enzyme values that may be elevated are usually limited to alanine aminotransaminase (ALT) and aspartate aminotransaminase (AST). The decision to look for hepatic steatosis must therefore be made on the basis of a number of risk factors, including elevated ALT or AST, if present, as well as obesity and other components of metabolic syndrome.

Biopsy

Tissue biopsy remains the gold standard for diagnosis and quantification of hepatic steatosis. There are multiple methods of obtaining hepatic tissue, including percutaneous, transjugular, laparoscopic, or ultrasound or CT-guided fine needle aspiration (FNA). Of these, percutaneous liver biopsies are the most common, as well as the fastest to perform, with ultrasound sometimes employed to identify a safe approach in high-risk patients. Ultrasound or CT-guidance is occasionally used to locate particular lesions of interest. Liver biopsy is considered a safe procedure, particularly when performed by experienced operators, with whom complications are quite rare (24). Medicare reimbursement for percutaneous liver biopsy is approximately $200, but the total cost, including use of hospital facilities, is approximately $1000.

Absolute contraindications to percutaneous liver biopsy include an uncooperative patient, a history of unexplained bleeding or a bleeding tendency which cannot be corrected with fresh-frozen plasma, unavailability of blood transfusion support, suspected hemangioma or vascular tumor, inability to identify an adequate

biopsy site by exam or ultrasound, and suspected echinococcal (hydatid cyst) disease. Relative contraindications are morbid obesity, ascites, hemophilia, and infection in the right pleural space or below the right hemidiaphragm (25).

Roughly one in four patients experiences significant pain following percutaneous liver biopsy. Other complications are rare, with significant complications occurring at a rate between 0.1 to 3.6% (26), and include bleeding, bile peritonitis, transient bacteremia, and perforation. The mortality associated with liver biopsy is very low, occurring at a rate of 1 in 10,000 to 12,000 procedures (27). While complications are unlikely, biopsy remains an invasive procedure and is not ideal for repeated sampling such as might be desired in monitoring disease progression or response to treatment, though serial biopsies are sometimes done. While significant hepatic steatosis, particularly once it has progressed to NASH, increases risk for cirrhosis and hepatocellular carcinoma, biopsy is not frequently performed to evaluate asymptomatic patients. Additionally, while it allows direct histological inspection of liver tissue, biopsy samples a small percentage of the total liver parenchyma. Fatty infiltration of the liver may be focal or diffuse, affecting different regions to differing degrees (28), leading to a risk of sample error. Also, interobserver variability may affect the reproducibility of results. Regardless of the potential for non-invasive methods of assessing hepatic steatosis, biopsy remains uniquely valuable in the assessment of other liver pathologies such as inflammation, fibrosis, necrosis, and iron deposition, though methods of iron detection using Magnetic Resonance imaging have been studied (29, 30).

Ultrasound

Ultrasound has been tested as a method of detecting and quantifying hepatic steatosis, and abdominal ultrasound is currently the most commonly used non-invasive method to evaluate for hepatic steatosis. Hyperechogenic liver tissue with fine, tightly packed echoes, hyperechoic relative to the adjacent right kidney or spleen on ultrasound examination is considered characteristic of liver steatosis. High frequency ultrasound was shown in one study to provide increased spatial resolution and better detail, but is limited by the difficulty of penetrating the abdominal wall (31). Duplex Doppler examination of hepatic veins may be useful in some cases, as fatty infiltration may cause abnormal waveforms by compression, however this effect does not appear to correlate with the degree of fatty infiltration (32).

Ultrasound may be the most sensitive non-invasive method of screening for fatty infiltration of the liver, though estimates vary between 60 and 95%, with specificity ranging between 84 and 100% (33, 34, 35). Ultrasound may miss low levels of steatosis (36), and it can be confused with the sonographic appearance of fibrosis, particularly when both fibrosis and steatosis are present. As with nearly any ultrasound exam, its usefulness to detect and quantify hepatic steatosis is operator dependent. In an effort to minimize observer bias, a grading system has been proposed, based on three sonographic features: liver echotexture, echo penetration, and clarity of blood vessels (33, 37, 38). In general, the low cost of ultrasound examination as well as the lack of radiation exposure and suitability for repeated examinations make it an attractive

option for screening for NAFLD, but it is non-quantitative and has limited ability to detect low levels of hepatic steatosis, though the consistent use of scoring systems may improve its quantitative abilities (35).

Computed Tomography

Computed Tomography (CT) imaging which includes part of all of the liver is frequently performed, including a large number of studies performed without specific concern for liver pathology such as hepatic steatosis. CT has the advantage over ultrasound of being quantitative and not as operator dependent. Given the high prevalence of hepatic steatosis in the general population, CT would be expected to incidentally reveal a significant number of otherwise unsuspected cases. Interest in the use of CT as a tool to screen for and quantify hepatic steatosis, particularly given its role in liver resection and transplantation, has led to a number of studies to determine its usefulness in this regard.

Liver attenuation is inversely correlated with the degree of fatty infiltration, though concurrent hemochromatosis, which tends to increase liver attenuation, can mask steatosis (39). Non-contrast enhanced CT appears to correlate better with histologic steatosis grade than contrast-enhanced imaging (40). A 2004 study of 42 patients compared the difference between liver and spleen attenuation values on non-contrast enhanced CT with histological fat percentage (41), and found that it was possible to correctly predict histologic grade in 90% of the subjects. However, nearly two-thirds of the subjects in that study had no significant fatty infiltration at all. This

study concluded that CT would preclude biopsy for only a small percentage of potential liver donors, and that histology was still valuable in screening for other conditions, such as hepatitis, fibrosis, and necrosis.

A 2006 study by Park et. al. used three indices of hepatic attenuation on unenhanced CT: liver-to-spleen ratio, liver minus spleen attenuation, and blood-free hepatic parenchymal attenuation (42). This last value was obtained by estimating bloodless attenuation of the liver with calculations that required measurement of attenuation in both the portal vein and hepatic artery. They concluded that there was no significant difference among these indices and that, while correlation with the degree of macrovesicular steatosis on biopsy was evident, the limits of agreement between histologic macrovesicular steatosis and each of these indices was too great to be of clinical use. A later study compared the biopsy correlation on non-contrast enhanced CT images of liver attenuation alone, liver minus spleen attenuation, and liver to spleen ratio, and concluded that while all had significant correlation with biopsy, simple measurement of liver attenuation was best for predicting liver fat content (40).

A recent study concerned with predicting adverse outcomes after liver resection demonstrated that liver minus spleen attenuation values on non-contrast CT for 26 patients demonstrated good sensitivity in detecting steatosis measured on biopsy but poor specificity, concluding that non-contrast CT could potentially be used to identify potential liver donors who should be biopsied (43), but was not otherwise useful in screening patients for hepatic steatosis.

The role of CT imaging of the liver remains controversial, with some studies demonstrating good correlation with biopsy results while others, particularly those measuring non-continuous biopsy indices such as hepatic steatosis grade, found that CT performed poorly in predicting significant hepatic steatosis. The confounding factor of variable iron content, which can offset the decrease in attenuation seen in fatty liver, led to a clearly decreased correlation in at least one study (44), making CT liver attenuation values unlikely to be helpful for patients with both excess iron and fatty infiltration.

Magnetic Resonance Imaging

The use of magnetic resonance imaging (MRI) to evaluate fat content of the liver in humans was reported in a study by Dixon, et. al. published in 1984 in *Radiology* describing the use of a modified spin echo technique (45). This study collected data on five subjects using a new technique that took advantage of the difference in rates of precession between protons in water and protons in fatty acid. This difference in rates of precession, and thus resonant frequency, is directly proportional to the main magnetic field strength and has been measured to be approximately 3.5 parts per million, which is a difference of about 225 Hertz at 1.5 Tesla. Using this technique, one image is acquired when water and fat magnetization are in-phase, that is, pointing the same direction, and another image when water and fat protons are out of phase, pointing in opposite directions, resulting in images that, when compared, can be used to indicate the proportion of a given tissue consisting of each component.

A 1991 study using 1.5-Tesla MR correlated fat fraction on MR with fat grade on biopsy for 16 subjects (46). This study used the same spin echo technique as the Dixon study in 1984 and showed good correlation between fat fraction on MR and histologic grade, particularly in individuals whose fatty infiltration on biopsy was less than 25%.

In a 2006 study, Kim et. al. (47) examined 57 potential liver donors by comparing biopsy and dual-echo 1.5-T MRI. Of these, 25 had no significant steatosis on biopsy, 23 had mild steatosis, 6 moderate, and 3 severe steatosis. The study used a calculation for relative signal intensity decrease (RSID) which included liver and spleen attenuation information. In this study, approximately 20% RSID corresponded to 30% macrosteatosis, which was that institution's cut-off of acceptability for liver donation. The study concluded that while MRI is unable to discriminate between microsteatosis and macrosteatosis, a RSID of 20% had 100% sensitivity and 92% specificity for screening donors with more than 30% macrosteatosis (47).

Statement of Purpose

The purpose of this study was to chart retrospective, unenhanced CT liver and spleen attenuation data on patients with normal and fatty livers to demonstrate a relationship between liver fat content and attenuation on unenhanced CT using MR chemical shift imaging as a reference standard.

Hypothesis

Unenhanced CT imaging of the liver, using liver attenuation, liver minus spleen, liver to spleen ratio, or a combination of these values can be used to predict hepatic steatosis as defined on opposed-phase magnetic resonance imaging by a relative signal intensity decrease of 20% or greater.

Specific Aims

1. Investigate the clinical relevance of hepatic steatosis, including that of its role in liver transplantation, and current methods of diagnosis and treatment.

2. Compare previously described imaging methods, including ultrasound, computed tomography and magnetic resonance imaging methods of detecting and quantifying hepatic steatosis and their accuracy in comparison with the gold standard of biopsy.

3. Chart retrospective, unenhanced CT liver and spleen attenuation data on patients with normal and fatty livers to demonstrate a relationship between MR liver fat content on opposed phase imaging and unenhanced CT liver attenuation, CT liver minus spleen, and CT liver/spleen ratio.

4. Perform statistical analysis to obtain a value or combination of factors that will predict the degree of fatty infiltration on unenhanced CT with optimal sensitivity and specificity.

Methods

This project was conceived by Richard Do, MD, a fourth year resident in Diagnostic Radiology at New York University Medical Center. Portions of this investigation done by Dr. Do, the author, or both are specified in the sections below.

Study Approval

Dr. Do wrote and submitted a protocol for this study which was approved by the institutional review board of NYU Medical Center. The patient consent requirement was waived for this retrospective chart review.

Study Location

All data were collected from the PACS database of Tisch hospital, an affiliate of New York University Medical Center, and included scans done at Tisch hospital (NYUMC-

TH), Faculty Practice Outpatient Office (NYUMC-FPO), and the Columbus Medical Institute.

Preliminary Data

To test the feasibility of obtaining useful data, Dr. Do collected information on fifteen patients who had been scanned at one of the above locations between April and September of 2007. Inclusion and exclusion criteria, as described for patients whose scans included mention of fatty liver, were used for this preliminary data set. Data on an additional four patients were gathered by the author in order to increase the number of borderline fatty livers, as defined by a CT mean attenuation value between 40 and 50, and project the feasibility of the study.

Study Population

We retrospectively reviewed our hospital database for patients who underwent both a CT with non contrast-enhanced images of the liver and also a non contrast-enhanced MR which included opposed-phase images of the liver within 60 days of each other. One data set included all patients who underwent both scans during the six month period from March to August 2007. In order to obtain more data on patients with significant hepatic steatosis, a second set of patients were reviewed which included all patients who underwent both scans within 60 days of each other, with at least one

report mentioning fatty liver, during the two year period from September 2005 through September 2007. Patients were excluded if the report mentioned liver metastases, a known history of hepatic cirrhosis or cirrhotic morphology. Data on a given patient was used only once, with patients included in the first set being excluded from the second. In cases where more than one scan was available for comparison within the specified 60-day period, the scan with the smallest time interval between was used, with the most recent studies preferred if time intervals were identical.

Data Collection

Data on CT attenuation and MR signal intensity, including placement of ROIs, were collected by the author, while additional information concerning the specific scanners used for each CT and MR scan, and data on MR image acquisition parameters such as TR and TE were later added by Dr. Richard Do, MD.

Computed Tomography

Computed Tomography Scans were performed on Sensation 16 (n=98), 40 (n=2), or 64 (n=12) slice or Somatom Definition dual-source (n=4) Seimens machines. Data were collected on CT scans of the chest, abdomen, or combined scans as long as sufficient images of the liver and spleen were included on a non-contrast enhanced series. For each patient, the attenuation from four regions of interest (ROIs) in the liver

and one ROI in the spleen were collected. ROIs were circular with a diameter of approximately 1 -2cm. Four ROIs were obtained in the mid-plane of the liver with one ROI each from Couinaud segments 2/3, 4A/4B, 8/5, and 7/6. ROIs were placed peripherally and with effort to avoid visible blood vessels and bile ducts. One, central splenic ROI was obtained on the same slice as the liver ROIs with the exception of 2 patients on whom the spleen was not visible in this slice. In these two cases, a splenic ROI was obtained several slices away where the spleen was sufficiently wide in cross-sectional area to accommodate it. For each patient, three different liver attenuation indices were obtained. Liver attenuation was calculated as the arithmetic mean of the four ROI values. Liver minus spleen (L-S) was calculated as the splenic attenuation subtracted from the mean liver attenuation value. Liver to spleen ratio (L/S) was calculated as the mean liver attenuation divided by the splenic attenuation.

Magnetic Resonance Imaging

Magnetic resonance imaging was performed on Avanto, Sonata Vision, Symphony, and Numaris 1.5 T scanners. Data were collected on scans which provided images through the mid-plane of the liver on in-phase and opposed-phase image series using either a body or torso coil. Slice thickness varied from 3 to 5mm, and echo times (TE) ranged from 1.99 to 2.40ms for opposed-phase and 4.76 to 4.97ms for in-phase images.

ROIs were selected to match as closely as possible those selected for CT. Four ROIs were obtained in the liver, at a level just superior to the left portal vein with one ROI each from Couinaud segments 2/3, 4A/4B, 8/5, and 7/6. ROIs were placed peripherally, avoiding visible blood vessels and bile ducts as well as areas affected by motion artifact. To ensure comparison was made between identical regions on both phases of imaging, once ROIs were chosen on one phase of the scan and their values recorded, they were left in place while the image was scrolled to the equivalent slice of the other phase to record the new values. For calculations, the mean of the four liver ROI values for each phase was used. A single central splenic ROI was obtained in each phase on the same slice as the liver ROIs, again leaving the ROI in place for both in- and out-of-phase attenuation values.

MRI fat fraction (MR FF) was equal to the percentage signal decrease on opposed-phase images relative to in-phase images calculated using the following formula:

$$\text{MR FF} = \%\ \text{signal decrease} = 100 * (L_{in}/S_{in} - L_{op}/S_{op})/(L_{in}/S_{in})$$

where L_{in} and S_{in} stand for signal intensity on in-phase images of the liver and spleen, respectively, and L_{op} and S_{op} stand for signal intensity on opposed-phase images of the liver and spleen, respectively (47).

Statistical Analysis

To determine whether non-contrast enhanced CT could predict degree of hepatic steatosis on opposed-phase MRI as determined by the percent signal decrease equation given above, MR FF was correlated with three potential measures of hepatic steatosis on CT: liver attenuation, liver minus spleen, and liver to spleen ratio, linear regression analysis was performed between the MR FF and each of these attenuation indices. Regression equations for each index were calculated, as well as 95% confidence intervals.

To compare the relative performance of these three indices for the quantification of steatosis, receiver operating characteristic (ROC) analysis was performed using the cutoff of 20% MR signal decrease, with the area under each curve calculated and compared for statistical differences among indices. Cutoff values for each attenuation index which optimized sensitivity and specificity were calculated from the ROC curve. Linear regression, confidence intervals, and ROC analysis was performed by Dr. Lawrence Staib, PhD, in the Diagnostic Radiology Department of Yale New Haven Hospital.

For each index, I determined the highest cutoff value that yielded 100% specificity for detection of MR FF of 0.2 or greater was determined. Sensitivity and specificity for each cutoff value was calculated.

Results

We obtained data on 75 patients in the March to August 2007 data set and 45 patients in the January 2005 through August 2007 data set, on patients with mention of fatty infiltration of the liver, for a total of 120 patients. Of these, four were eliminated after data collection because the MR opposed phase imaging had inappropriately high TE values of 2.8-4.76ms (opposed-phase) and 5.13-11.9ms (in-phase). This left data on 116 patients, which was used for all subsequent data analysis (Table 1).

Pt number[a]	Age (yr)[b]	Days Between Imaging Studies	Liver Attenuation (H)[c]	Spleen Attenuation (H)[d]	Liver minus Spleen (H)	Liver / Spleen ratio	MR Fat fraction (RSID)
1000	56	0	57.7	50.4	7.3	1.14	-0.01
1001	52	0	59.8	53.7	6.1	1.11	0.21
1002	77	0	58.9	43.4	15.6	1.36	-0.03
1003	65	14	46.9	47.4	-0.5	0.99	0.38
1004	68	16	57.6	48.4	9.2	1.19	0.02
1005	50	14	49.1	57.2	-8.1	0.86	0.37
1006	58	0	65.9	44.7	21.2	1.47	-0.05

Pt number[a]	Age (yr)[b]	Days Between Imaging Studies	Liver Attenuation (H)[c]	Spleen Attenuation (H)[d]	Liver minus Spleen (H)	Liver / Spleen ratio	MR Fat fraction (RSID)
1007	78	13	62.9	45.1	17.8	1.40	-0.06
1008	72	32	65.0	43.7	21.2	1.49	-0.05
1009	82	22	51.2	51.2	0.0	1.00	0.15
1010	72	0	57.3	44.0	13.2	1.30	-0.16
1011	85	15	54.6	45.3	9.2	1.20	-0.09
1012	77	0	64.8	54.0	10.8	1.20	-0.10
1013	75	0	58.5	55.0	3.6	1.07	0.14
1014	70	9	56.2	48.6	7.6	1.16	0.06
1015	50	21	54.9	50.9	4.1	1.08	0.02
1016	58	16	72.5	50.9	21.6	1.42	-0.16
1017	69	19	68.3	47.7	20.6	1.43	-0.07
1018	60	15	62.0	46.3	15.6	1.34	0.01
1019	60	61	56.2	38.3	17.9	1.47	-0.06
1020	61	4	56.2	47.2	9.0	1.19	0.09
1021	71	0	42.4	52.3	-9.9	0.81	0.29
1022	55	0	66.9	53.9	13.0	1.24	0.14
1023	68	0	41.9	41.9	0.0	1.00	0.17
1024	85	0	57.8	48.3	9.5	1.20	-0.20
1025	29	48	53.4	50.0	3.4	1.07	-0.02
1026	75	37	53.9	51.1	2.8	1.05	0.03
1027	55	26	66.5	49.4	17.1	1.35	0.07
1028	53	5	67.4	45.4	22.0	1.48	-0.11
1029	74	6	66.2	49.4	16.8	1.34	-0.06

Pt number[a]	Age (yr)[b]	Days Between Imaging Studies	Liver Attenuation (H)[c]	Spleen Attenuation (H)[d]	Liver minus Spleen (H)	Liver / Spleen ratio	MR Fat fraction (RSID)
1030	83	0	59.0	45.4	13.6	1.30	0.01
1031	76	0	39.8	56.4	-16.6	0.71	0.41
1032	72	22	61.6	52.8	8.9	1.17	0.00
1034	80	0	61.9	48.1	13.8	1.29	0.00
1035	80	0	61.0	46.7	14.3	1.31	-0.05
1036	62	0	56.1	50.4	5.7	1.11	0.08
1037	62	42	42.5	46.8	-4.3	0.91	0.36
1038	88	0	56.4	44.3	12.1	1.27	-0.08
1039	67	14	30.4	45.8	-15.4	0.66	0.62
1040	82	0	64.6	49.5	15.1	1.31	-0.12
1041	55	24	15.2	51.5	-36.3	0.30	0.59
1042	55	23	30.2	49.2	-19.0	0.61	0.55
1043	81	8	66.0	48.8	17.3	1.35	-0.07
1044	60	0	56.9	49.9	7.1	1.14	-0.07
1045	68	0	58.7	53.7	5.1	1.09	0.00
1046	69	16	67.6	52.0	15.6	1.30	0.04
1047	67	8	45.8	46.1	-0.4	0.99	0.06
1048	58	0	46.5	48.5	-2.0	0.96	0.15
1049	64	0	59.8	50.3	9.4	1.19	0.07
1050	46	16	49.7	48.1	1.6	1.03	0.09
1051	52	8	52.9	47.1	5.8	1.12	-0.02
1052	88	0	51.9	43.7	8.2	1.19	0.02
1053	68	0	60.9	54.0	6.9	1.13	0.13

Pt number[a]	Age (yr)[b]	Days Between Imaging Studies	Liver Attenuation (H)[c]	Spleen Attenuation (H)[d]	Liver minus Spleen (H)	Liver / Spleen ratio	MR Fat fraction (RSID)
1054	69	0	37.0	46.8	-9.8	0.79	0.48
1055	54	41	63.4	52.3	11.1	1.21	0.08
1056	59	0	55.9	43.5	12.5	1.29	-0.06
1057	78	36	44.0	40.8	3.2	1.08	0.03
1058	82	0	59.0	54.9	4.1	1.07	0.04
1059	81	0	62.9	48.6	14.4	1.30	-0.05
1060	84	1	52.7	50.2	2.5	1.05	0.20
1061	95	0	61.5	47.3	14.2	1.30	0.02
1062	78	0	36.3	53.7	-17.4	0.68	0.64
1063	42	18	54.2	45.2	9.0	1.20	-0.04
1064	52	26	67.1	49.2	17.9	1.36	-0.07
1065	40	33	64.7	49.2	15.5	1.32	-0.10
1066	85	23	56.3	49.4	6.9	1.14	-0.10
1067	75	3	64.8	47.1	17.7	1.38	0.03
1068	58	25	57.2	53.3	3.9	1.07	0.00
1069	58	2	50.1	38.6	11.5	1.30	-0.11
1071	59	28	37.2	48.6	-11.4	0.77	0.39
1072	83	0	59.2	52.8	6.4	1.12	0.06
1073	74	0	60.2	44.9	15.3	1.34	-0.06
1074	57	3	61.8	49.5	12.3	1.25	0.14
2001	98	0	42.7	52.2	-9.5	0.82	0.47
2002	41	56	45.6	48.1	-2.6	0.95	0.30
2003	61	42	47.4	51.9	-4.4	0.91	0.27

Pt number[a]	Age (yr)[b]	Days Between Imaging Studies	Liver Attenuation (H)[c]	Spleen Attenuation (H)[d]	Liver minus Spleen (H)	Liver / Spleen ratio	MR Fat fraction (RSID)
2004	61	1	53.7	47.3	6.3	1.13	0.26
2005	67	4	40.7	41.2	-0.5	0.99	0.38
2006	61	0	41.0	47.5	-6.6	0.86	0.35
2007	34	0	24.2	47.8	-23.6	0.51	0.60
2009	62	0	24.8	50.8	-26.0	0.49	0.54
2010	58	33	48.4	47.7	0.7	1.01	0.27
2011	70	25	38.4	46.5	-8.1	0.83	0.38
2012	68	6	36.8	50.7	-13.9	0.73	0.41
2013	35	0	22.8	57.7	-34.9	0.40	0.76
2014	69	28	41.9	48.9	-7.0	0.86	0.25
2015	74	0	43.4	45.1	-1.7	0.96	0.23
2016	68	0	44.7	47.5	-2.8	0.94	0.37
2017	66	0	47.3	55.0	-7.7	0.86	0.30
2018	43	0	27.0	51.2	-24.3	0.53	0.58
2019	47	15	24.7	55.8	-31.1	0.44	0.64
2020	65	0	32.4	50.7	-18.3	0.64	0.54
2021	43	29	29.4	47.5	-18.0	0.62	0.59
2022	58	8	46.5	60.4	-13.9	0.77	0.41
2023	38	5	43.0	46.8	-3.7	0.92	0.23
2024	60	8	51.5	42.5	9.0	1.21	0.11
2025	79	0	46.3	47.8	-1.6	0.97	0.25
2026	21	0	49.9	53.5	-3.6	0.93	0.20
2027	50	48	35.0	44.6	-9.5	0.79	0.65

Pt number[a]	Age (yr)[b]	Days Between Imaging Studies	Liver Attenuation (H)[c]	Spleen Attenuation (H)[d]	Liver minus Spleen (H)	Liver / Spleen ratio	MR Fat fraction (RSID)
2029	53	7	49.1	51.9	-2.8	0.95	0.30
2030	83	29	53.5	48.1	5.4	1.11	0.04
2031	66	16	35.8	47.1	-11.2	0.76	0.39
2032	67	0	41.4	50.3	-8.9	0.82	0.26
2033	67	0	34.2	53.9	-19.7	0.64	0.46
2034	48	29	45.7	52.6	-7.0	0.87	0.27
2035	71	0	41.8	50.6	-8.8	0.83	0.48
2036	32	51	49.2	52.8	-3.6	0.93	0.19
2037	70	47	44.8	51.1	-6.3	0.88	0.17
2038	67	14	30.2	47.3	-17.0	0.64	0.59
2039	60	0	46.1	50.0	-3.9	0.92	0.32
2040	75	24	53.3	54.7	-1.4	0.98	0.22
2041	63	0	48.2	51.6	-3.4	0.93	0.20
2042	53	0	38.9	42.8	-3.9	0.91	0.28
2043	68	10	36.1	48.5	-12.4	0.74	0.40
2044	78	6	39.9	39.0	1.0	1.02	0.32
2045	50	12	55.2	47.0	8.2	1.18	0.07

Table 1: Data obtained on a total of 116 patients.

[a]Pt number is the patient number assigned for this study. Patient numbers from 1000 to 1074 refer to patient data gathered from the six-months of March – August, 2007; Patient numbers from 2001 to 2045 refer to patient data gathered on scans from January 2005 to August 2007 on patients with reference to fatty infiltration of the liver.

[b]Age is given at the time of the CT scan.

[c]Liver attenuation is the mean value of the 4 ROIs obtained on CT.

[d]Spleen attenuation on CT.

[e]Liver minus spleen, Liver to spleen ratio, and MR fat fraction (RSID) were calculated as described in Methods.

These patients ranged in age from 21 to 98 years old, with a mean age of 64 and standard deviation of 14 years (Figure 1). The time interval between the CT and MRI scans ranged between 0 and 61 days, with a mean of 12 days and a standard deviation of 15 days.

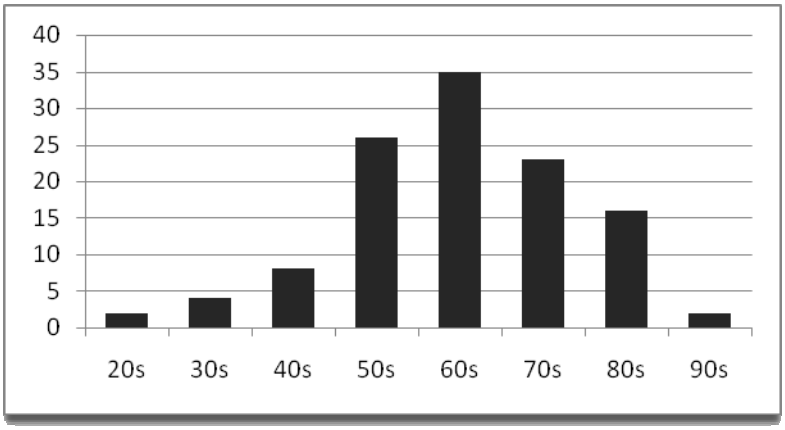

Figure 1: Age distribution of all patients analyzed in this study, by decade.

Computed Tomography

Liver attenuation values ranged from 15 to 73 Hounsfield units, with the breakdown shown in Figure 2. The difference between liver and spleen values varied from -36 to +22 Hounsfield units; the breakdown is shown in Figure 3. The liver to spleen ratio varied from 0.3 to 1.5, with the breakdown shown in Figure 4.

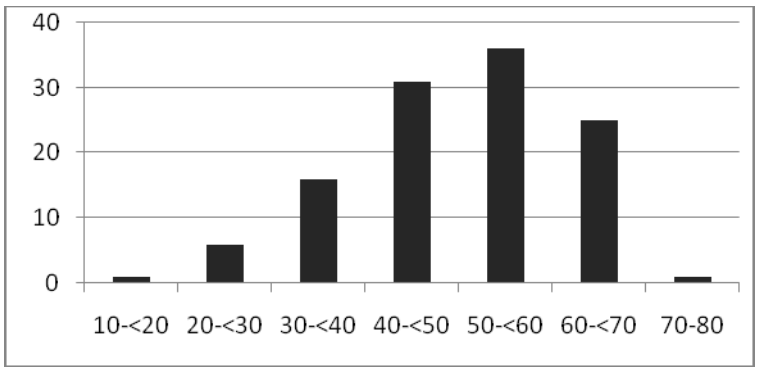

Figure 2: Number (y-axis) of all patients within the specified ranges with liver attenuation values (x-axis), in Hounsfield units, on unenhanced CT.

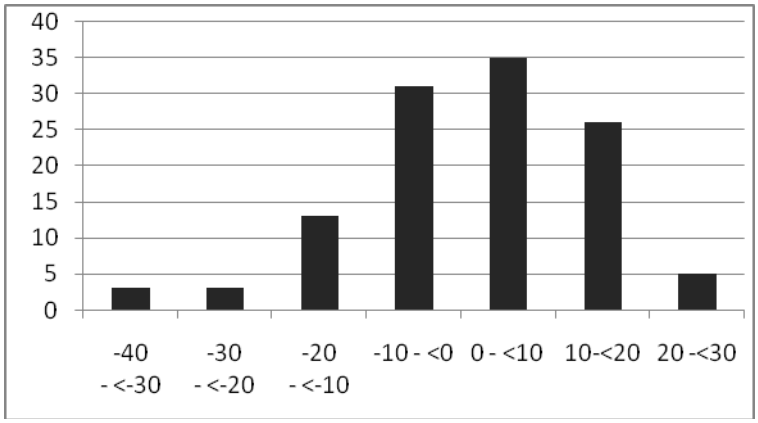

Figure 3: Number (y-axis) of all patients within the specified ranges of liver minus spleen attenuation values (x-axis), in Hounsfield units, on unenhanced CT.

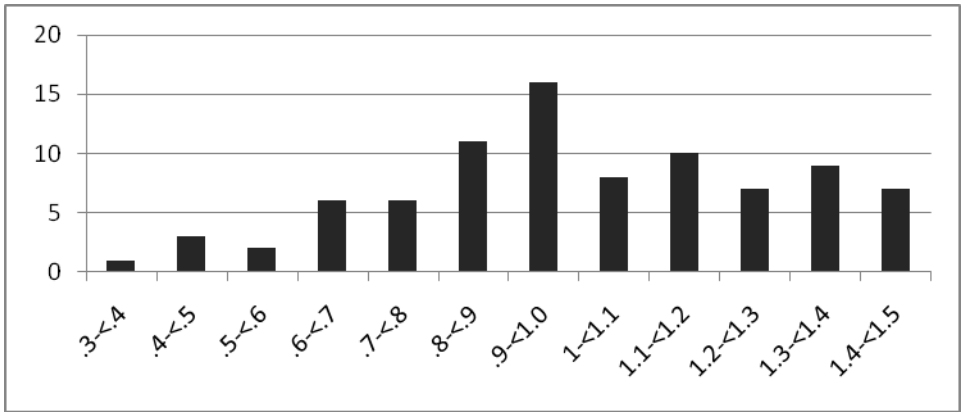

Figure 4: Number (y-axis) of all patients within the specified ranges of liver to spleen ratio (x-axis), in Hounsfield units, on unenhanced CT.

Magnetic Resonance Imaging

The signal decrease seen using opposed phase MR imaging was from -.20 to +.76, show with breakdown in Figure 5.

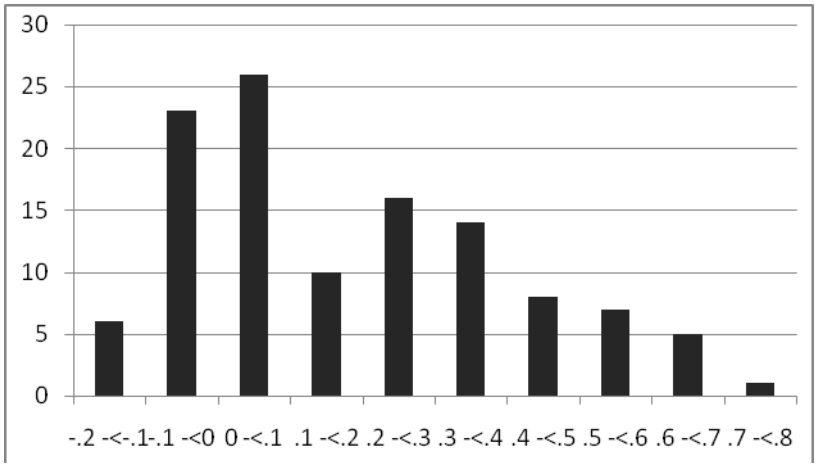

Figure 5: Number (y-axis) of all patients within the specified ranges of MR opposed phase imaging signal decrease or fat fraction (x-axis).

Comparison Between CT and MR

Linear regression analysis results between Magnetic Resonance fat fraction (MR FF) and CT liver attenuation, liver minus spleen attenuation, and liver to spleen ratio are presented in scatter plots (Figures 6, 7, 8). The linear regression equation that was used to quantitatively estimate the degree of steatosis using CT liver attenuation is: MR FF = 1.03 – 0.0169 * (liver attn). The linear regression equation that was used to quantitatively estimate the degree of steatosis using the difference between liver and spleen attenuation (L-S diff) is: MR FF = 0.198 – 0.0162 * (L-S diff). The linear regression

equation that was used to quantitatively estimate the degree of steatosis using the ratio of liver and spleen attenuation (L/S ratio) is: MR FF = 1.00 – 0.799 * (L/S ratio).

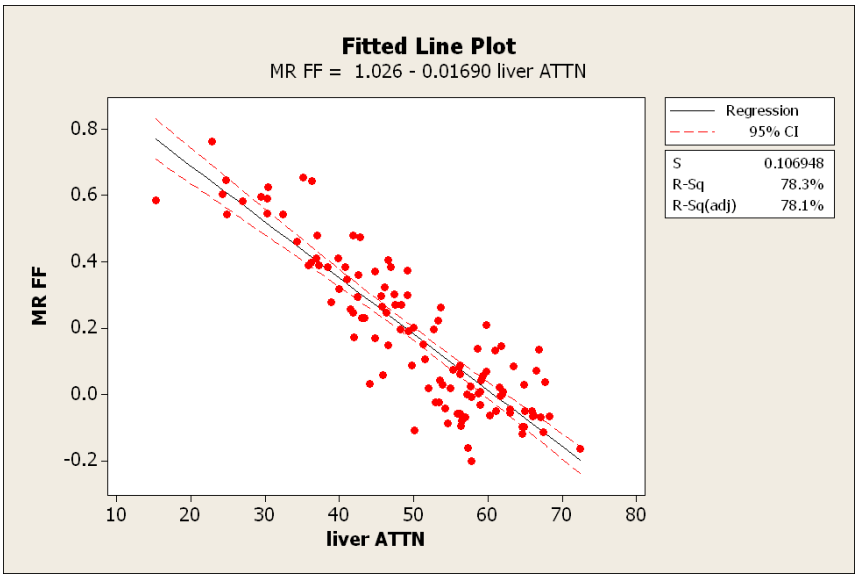

Fig 6: Scatter plot of liver attenuation (liver ATTN) on CT versus Magnetic Resonance fat fraction (MR FF). Best fit line is shown as a solid line and 95% confidence intervals are represented by dotted lines above and below the best fit line.

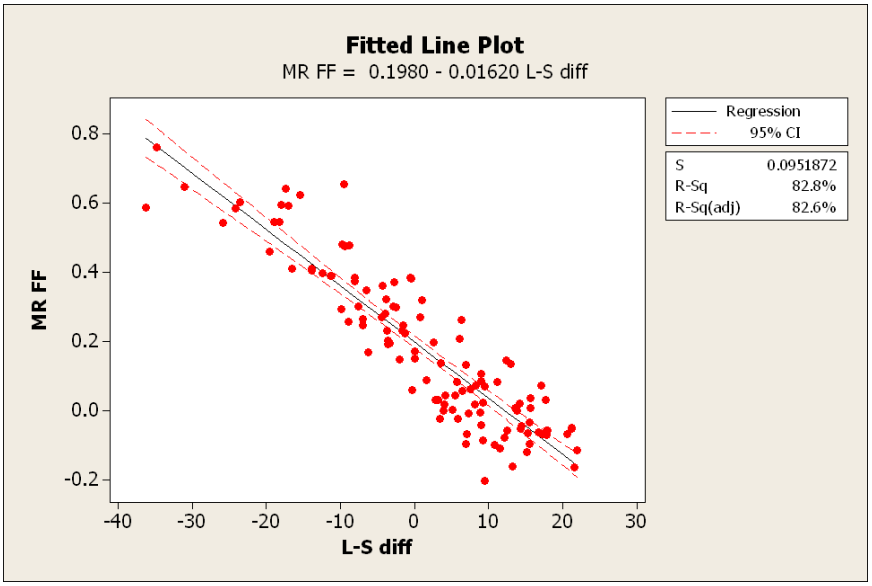

Figure 7: Scatter plot of liver minus spleen difference (L-S diff) on CT versus Magnetic Resonance fat fraction (MR FF). Best fit line is shown as a solid line and 95% confidence intervals are represented by dotted lines above and below the best fit line.

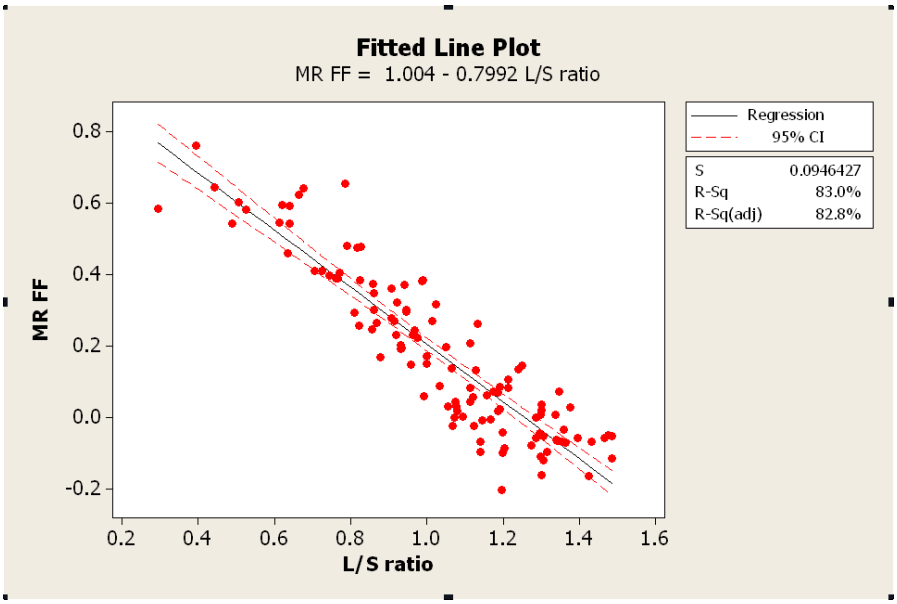

Figure 8: Scatter plot of liver to spleen ratio (L/S ratio) on CT versus Magnetic Resonance fat fraction (MR FF). Best fit line is shown as a solid line and 95% confidence intervals are represented by dotted lines above and below the best fit line.

The distribution of patients who had a MR FF of at least 20% or of less than 20% using each CT index by range is shown in figures 9, 10, and 11 below.

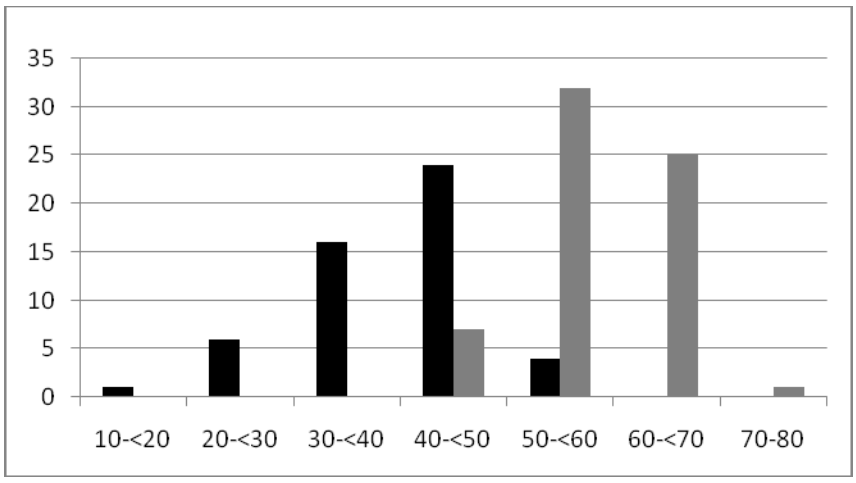

Figure 9: CT liver attenuation values (x-axis) of patients found by MR opposed-phase imaging to have a Magnetic Resonance fat fraction (MR FF) of 20% or greater (black bars) or less than 20% (grey bars) by number of patients (y-axis) in each specified range.

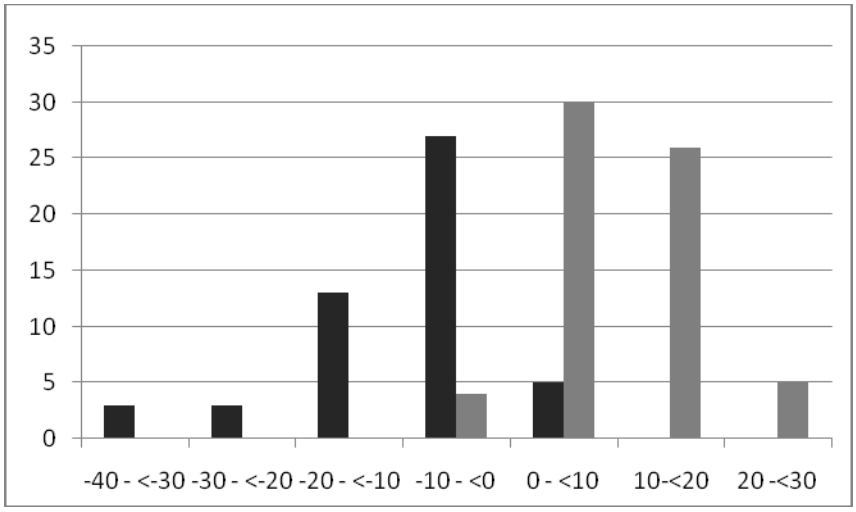

Figure 10: CT liver minus spleen values (x-axis) of patients found by MR opposed-phase imaging to have a Magnetic Resonance fat fraction (MR FF) of 20% or greater (black bars) or less than 20% (grey bars) by number of patients (y-axis) in each specified range.

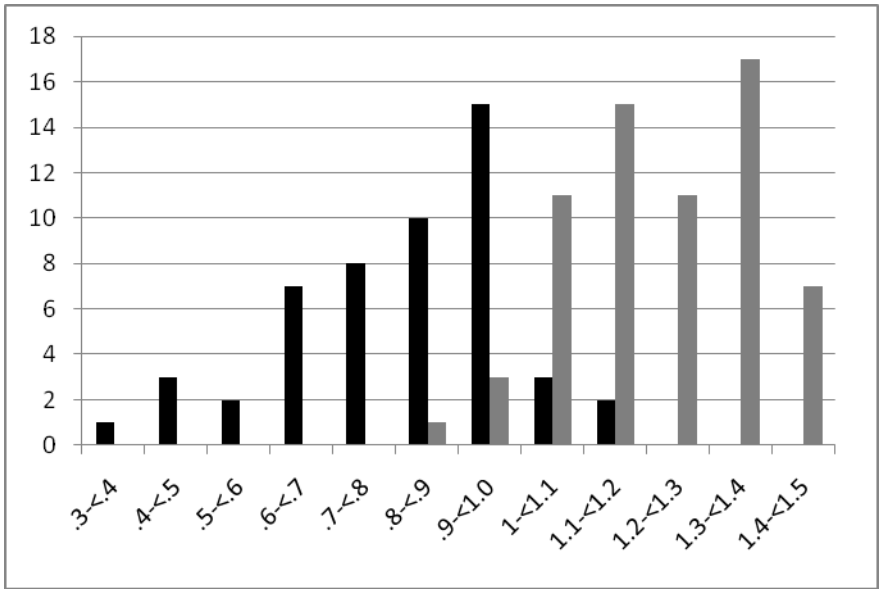

Figure 11: CT liver to spleen ratios (x-axis) of patients found by MR opposed-phase imaging to have a Magnetic Resonance fat fraction of 20% or greater (black bars) or less than 20% (grey bars) by number of patients (y-axis) in each specified range.

ROC Curve Analysis

The area under the ROC curve for MR FF of 0.2 (20%) or greater was 0.958 for liver attenuation alone, 0.973 for liver minus spleen, and 0.972 for liver to spleen ratio. There was no statistically significant difference among these indices. The cutoff value that provided a balance between sensitivity and specificity for the MR FF of 0.2 or greater was 49.2 H for liver attenuation alone, 0 (no difference) for liver minus spleen, and 1.0 for liver to spleen ratio. Sensitivity and specificity for liver attenuation less than 49.2 H were 91% and 92%, respectively. A cutoff of 0 for liver minus spleen also had a sensitivity and specificity of 91% and 92%, respectively. Liver to spleen ratio of 1.0 or less had a sensitivity and specificity of 93% and 92%, respectively (Table 2). The ROC curves generated for each index are seen in Figures 12, 13 and 14.

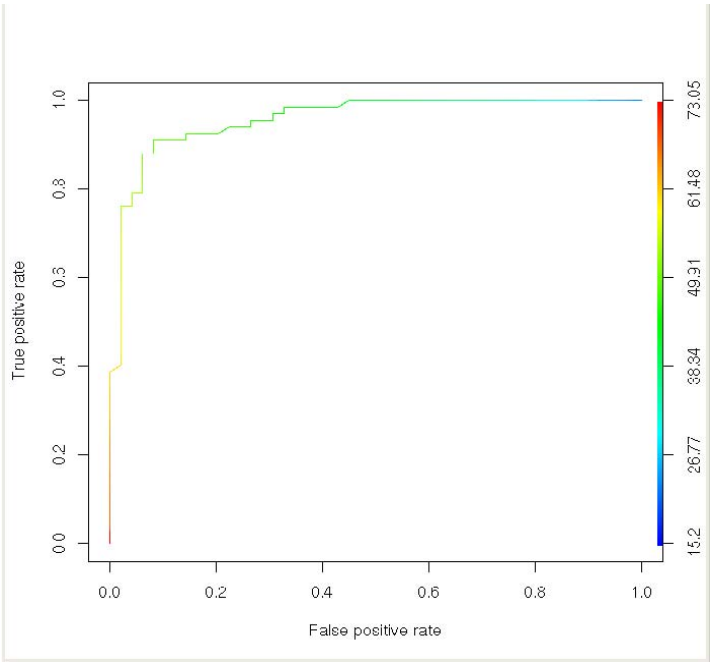

Figure 12: Liver ROC curve

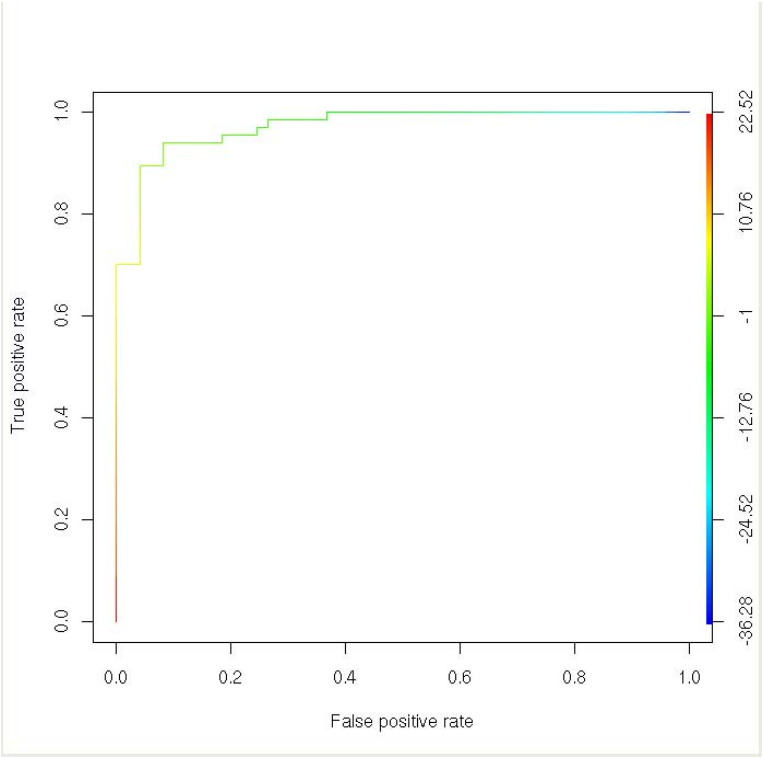

Figure 13: L-S ROC curve

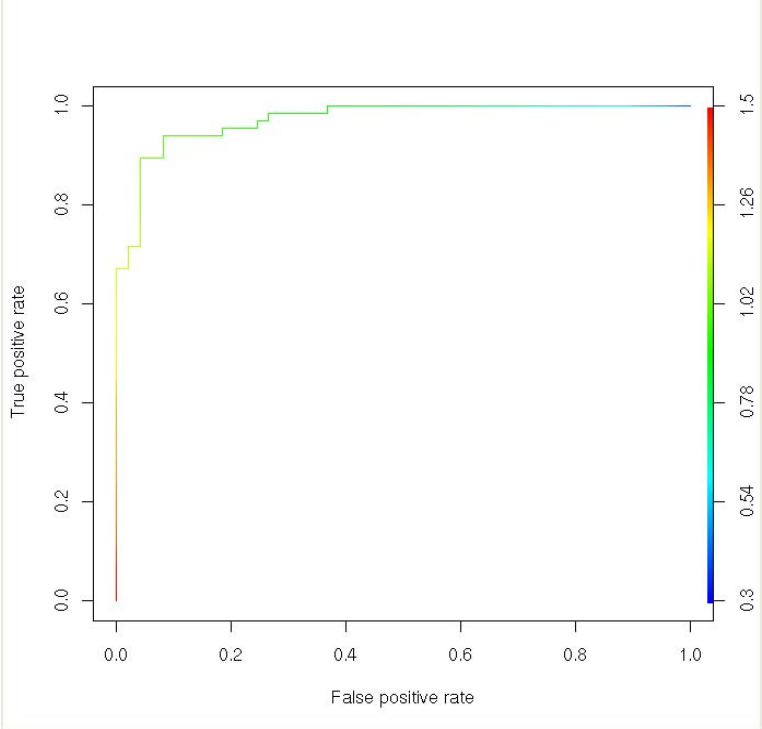

Figure 14: L/S ROC curve

CT index	Area under ROC curve	Cutoff value for MR FF 0.2	Sensitivity	Specificity
Liver attenuation	0.958	49.2	91%	92%
Liver minus spleen	0.973	0	91%	92%
Liver to spleen ratio	0.972	1.0	93%	92%

Table 2: Summary of ROC analysis

The highest cutoff value, in Hounsfield units, that was 100% specific in detecting a MR FF of 0.2 or greater using liver attenuation alone was 42, giving a sensitivity of 55%. The highest cutoff value for liver minus spleen attenuation that was 100% specific in detecting a MR FF of 0.2 or greater was -6.6, with a specificity of 61%. The highest cutoff value for liver to spleen ratio that was 100% specific in detecting a MR FF of 0.2 or

greater was 0.87, with a sensitivity of 61%. Positive and negative predictive values were not calculated, as the prevalence and distribution of fatty infiltration in the patients studied was not reflective of rates in the general population.

Discussion

Correlation

This analysis showed good correlation between MR fat fraction and each of the three CT indices studied. As there is no statistical difference in the accuracy of liver attenuation alone, liver minus spleen attenuation, and liver to spleen ratio, it is likely that liver attenuation alone may be the simplest, and therefore most convenient and likely to be used, index in determining hepatic fat content. Other studies have used the more complicated method of determining liver parenchymal attenuation, which requires measurement of hepatic artery and portal vein attenuation, and the use of an equation (47). As this method was not found to be statistically more useful than liver minus spleen difference or liver to spleen ratio, and in this study liver attenuation was as accurate as these other two indices, it is unlikely that additional information is gained from time taken to record and calculate extra measurements. Also, this method can be used on both chest and abdominal non-contrast CT images. In a chest CT, the liver is rarely fully imaged, and these studies may not obtain a good view of the hepatic artery.

Magnetic Resonance Imaging

While magnetic resonance imaging is not the gold standard for detection and quantification of hepatic steatosis, several studies have shown good correlation between signal decrease on opposed phase magnetic resonance imaging and histologic fat percentage (47, 48). Magnetic resonance imaging provides information on morphology and a geographic representation of the fat distribution of the liver and avoids certain potential problems of biopsy such as sampling error and interobserver variability. However, it does not discriminate between microsteatosis and macrosteatosis. To the extent that this distinction is clinically useful, as many studies on living liver donor transplantation have suggested, MR imaging alone is not ideal for determining donor candidate appropriateness, but may be useful in screening out, and thus preventing the unnecessary biopsy of, certain candidates who are clearly above the cutoff. This study demonstrates that CT may have similar usefulness, in that liver attenuation above or below certain extreme cutoffs may be sufficient to rule out or rule in significant hepatic steatosis. In this study, liver attenuation below 42 H was always associated with an MR FF of 0.2, corresponding to at least 30% macrosteatosis (47), while attenuation of 60 H or greater always corresponded to an MR FF of less than 0.2. While this leaves a considerable zone of overlap between 42 and 60 H, the high sensitivities and specificities given for the liver attenuation cutoff of 50 H optimized by ROC curve analysis are reasonable for clinical use. Also, this study established that there

is a linear correlation between MR FF and CT attenuation. The cutoff of MR FF of 0.2 was chosen because it was shown to correspond to 30% macrosteatosis, a cutoff for acceptability in living donor liver transplant. This, then, is already a very significant amount of hepatic steatosis, and it is reasonable that clinicians might be interested in detecting and monitoring considerably lesser degrees of steatosis.

Aside from its applicability to liver surgery, particularly liver transplantation, the detection of various degrees of hepatic steatosis using a non-invasive diagnostic test may be useful in clinical practice, particularly in caring for patients with NAFLD or NASH. High-end estimates of the prevalence of hepatic steatosis are above one-third of the general population, and this number is expected to increase, given increasing rates of obesity and metabolic syndrome, so that the average value of liver attenuation on CT may not represent the ideal. There is a linear relationship between CT attenuation and hepatic steatosis by MR, from which it may be understood that some steatosis of some significant degree is likely present in most patients with liver attenuation values in the 40s, and even many between 50 and 60. Even when CT of the liver is not done with hepatic steatosis in mind, it may be used to follow liver attenuation values to get some sense of the level of steatosis and to follow its trend, though the accuracy of this use has not been tested.

Limitations

The amount of time between each patient's MR and CT was ranged from zero up to 61 days (2 months). Ideally, studies done the same day would be compared, but this range was thought to reflect a balance between the usefulness of additional data points and the need to minimize the chances that the actual degree of hepatic steatosis had changed in the interval. Previous studies comparing biopsy to either MR imaging or CT have been limited by the number of patients undergoing biopsy to less than 60. This study was able to analyze nearly twice that number by taking advantage of the large amount of retrospective data available on patients who had undergone both unenhanced CT and opposed-phase MR of the liver as part of their clinical care.

MR opposed phase imaging is limited by ambiguity error, as it is not possible to know whether fat or water is providing the dominant signal. In cases where the fat fraction is greater than the water fraction, opposed-phase imaging could underestimate the amount of hepatic steatosis. In one study looking at hepatic fat by biopsy and MR opposed-phase imaging, there were no instances of inappropriate signal intensity increases, despite having biopsy fat fractions as high as 81% (47). The correlation seen in this study also appears to continue through the highest fat fractions. Also, hepatic steatosis of more than 50% is a relatively rare event, so this may not cause confusion between patients with low fat fractions and those with exceedingly high fat fractions in clinical practice; as this study did not include biopsy results, this cannot be ruled out. A different MRI technique called iterative decomposition of water and fat with echo

asymmetry and least squares estimation (IDEAL), is able to separate water and fat signals, and can be used to overcome this problem (49). However, this is less frequently performed than opposed-phase imaging, and this study did not look at data using this technique.

The problem of determining hepatic iron content using non-invasive imaging, particularly when there is concurrent fatty infiltration, is still being investigated, and some techniques are promising (29, 30, 39). The incidence of iron overload is low, and this study did not attempt to detect or correct for high levels of iron, but the results may not be as useful if there was a significant incidence of iron overload in the population used and cannot be applied to patients with iron overload.

This study used data obtained on multiple CT scanners with varying slice numbers and thicknesses, technicians, and protocols. Similarly, MR data were obtained on several different scanners using slightly different parameters, though those with TE values outside the acceptable range were removed from the data set before analysis. While this could introduce some variability, it reflects the varying types of scans that a practicing radiologist might be expected to interpret.

Data were not collected on patients with evidence of cirrhosis or of widely metastatic disease. While cirrhotic morphology and metastases may be identified on imaging, it is unknown how applicable these results would be to patients with cirrhosis or metastatic disease.

Other Imaging Methods

One option proposed to evaluate hepatic steatosis accurately and non-invasively is the combination of two modalities such as ultrasound and MR imaging (47). Applying artificial neuronal networks to ultrasound increased its specificity over that of radiologists in detecting hepatic macrosteatosis over their institution's limit of eligibility for liver donation (50). Combinations of ultrasound and CT may increase the ability to detect levels of hepatic steatosis as well, given the excellent correlation between CT and MR results in this study.

Another magnetic resonance technique used to investigate the degree of fatty infiltration of the liver is ^{1}H magnetic resonance spectroscopy (MRS). This technique, rather than providing a visual representation of the geography of the liver, generates a spectrum of resonances which can, by comparing fat and water peaks, provide information on the relative amounts of fat present in a selected tissue volume of interest (VOI). One study analyzed fat and water on ^{1}H spectra on VOIs within the liver on MR spectroscopy and demonstrated good correlation of fatty infiltration with CT imaging and as well as with histological score (51). While the VOI used to evaluate hepatic steatosis is much greater than the tissue volume obtained by biopsy, inhomogeneity of fat distribution may still lead to incorrect estimates of the overall degree of fatty infiltration. Also, as this technique is not routinely performed as part of liver imaging using magnetic resonance imaging, the extra steps required to perform it and analyze the data make it less likely to be used in clinical practice at this time. A recent study investigated the use of iterative decomposition of water and fat with echo

asymmetry and least squares estimation (IDEAL) to overcome the limitation of MR in separating fat and water signals which can cause ambiguity error (49). Using a phantom, they were able to reduce the deviation of fat-fraction from its true value, particularly prominent at high fat-fractions. Once this technique has been demonstrated to be accurate in clinical studies it may represent a useful non-invasive alternative to biopsy or standard MR sequences.

References

1. Browning, J.D., Szczepaniak, L.S., Dobbins, R., Nuremberg, P., Horton, J.D., et. al. Prevalence of Hepatic Steatosis in an Urban Population in the United States: Impact of Ethnicity. Hepatology. 2004 Dec;40(6):1387-95.

2. Adams L.A., Angulo P. Recent concepts in non-alcoholic fatty liver disease. Diabet Med. 2005 Sep;22(9):1129-33.

3. Hilden M., Christoffersen P., Juhl E., Dalgaard J.B. Liver histology in a 'normal' population--examinations of 503 consecutive fatal traffic casualties. Scand J Gastroenterol. 1977;12(5):593-7.

4. Clark, J.M., Brancati, F.L., Diehl, A.M. Nonalcoholic Fatty Liver Disease. Gastroenterology 2002:122:1649-57.

5. Selzner M., Clavien P.A. Fatty liver in liver transplantation and surgery. Semin Liver Dis 2001; 21:105–113.

6. Tendler, D.A. Pathogenesis of nonalcoholic fatty liver disease. Up To Date. 2007. www.uptodateonline.com.

7. American Gastroenterological Association medical position statement: nonalcoholic fatty liver disease. Gastroenterology. 2002 Nov;123(5):1702-4

8. Luyckx FH, Desaive C, Thiry A, Dewé W, Scheen AJ, *et al.* Liver abnormalities in severely obese subjects: effect of drastic weight loss after gastroplasty. Int J Obes Relat Metab Disord. 1998 Mar;22(3):222-6.

9. Ranløv I, Hardt F. Regression of liver steatosis following gastroplasty or gastric bypass for morbid obesity. Digestion. 1990;47(4):208-14.

10. Capron JP, Delamarre M, Dupas JL, Bradlon A, Degott C. Fasting in obesity: another cause of liver injury with alcoholic hyaline? Dig Dis Sci 1982;54:374-377.

11. Miglio F, Rovati LC, Santoro A, Setnikar I. Efficacy and safety of oral betaine glucuronate in non-alcoholic steatohepatitis. A double-blind, randomized, parallel-group, placebo-controlled prospective clinical study. Arzneimittelforschung. 2000 Aug;50(8):722-7.

12. Marchesini G, Bnzl M, Bianchi G, Tomasselli S, Zoll M, *et al*. Metformin in non-alcoholic steatohepatitis. Lancet 2001;358:893-894.

13. Promrat K, Lutchman G, Uwaifo GI, Freedman RJ, Soza A, *et al*. A pilot study of pioglitazone treatment for nonalcoholic steatohepatitis. Hepatology. 2004 Jan;39(1):188-96.

14. Marsman WA, Wiesner RH, Rodriguez L, Batts KP, Porayko MK, *et al*. Use of fatty donor liver is associated with diminished early patient and graft survival. Transplantation. 1996 Nov 15;62(9):1246-51.

15. Markin RS, Wisecarver JL, Radio SJ, Stratta RJ, Langnas AN, *et al.* Frozen section evaluation of donor livers before transplantation. Transplantation. 1993 Dec;56(6):1403-9.

16. Charatcharoenwitthaya P, Lindor KD. Role of radiologic modalities in the management of non-alcoholic steatohepatitis. Clin Liver Dis. 2007 Feb;11(1):37-54, viii. Review.

17. Ureña MA, Ruiz-Delgado FC, González EM, Segurola CL, Romero CJ, *et al*. Assessing risk of the use of livers with macro and microsteatosis in a liver transplant program. Transplant Proc. 1998 Nov;30(7):3288-91.

18. Kooby DA, Fong Y, Suriawinata A, Gonen M, Allen PJ, *et al*. Impact of steatosis on perioperative outcome following hepatic resection. J Gastrointest Surg. 2003 Dec;7(8):1034-44.

19. Karoui M, Penna C, Amin-Hashem M, Mitry E, Benoist S, *et al*. Influence of preoperative chemotherapy on the risk of major hepatectomy for colorectal liver metastases. Ann Surg. 2006 Jan;243(1):1-7.

20. Fong Y, Bentrem DJ. CASH (Chemotherapy-Associated Steatohepatitis) costs. Ann Surg. 2006 Jan;243(1):8-9.

21. Vauthey JN, Pawlik TM, Ribero D, Wu TT, Zorzi D, *et al*. Chemotherapy regimen predicts steatohepatitis and an increase in 90-day mortality after surgery for hepatic colorectal metastases. J Clin Oncol. 2006 May 1;24(13):2065-72.

22. Fernandez FG, Ritter J, Goodwin JW, Linehan DC, Hawkins WG, *et al*. Effect of steatohepatitis associated with irinotecan or oxaliplatin pretreatment on resectability of hepatic colorectal metastases. J Am Coll Surg. 2005 Jun;200(6):845-53.

23. Clark JM, Brancati FL, Diehl AM. The prevalence and etiology of elevated aminotransferase levels in the United States. Am J Gastroenterol 2003;98:960–7.

24. Froehlich F; Lamy O; Fried M; Gonvers JJ. Practice and complications of liver biopsy. Results of a nationwide survey in Switzerland. Dig Dis Sci 1993 Aug;38(8):1480-4.

25. Bravo AA, Sheth SG, Chopra S. Liver biopsy. N Engl J Med 2001; 344:495.

26. Van Thiel DH, Gavaler JS, Wright H, Tzakis A. Liver biopsy. Its safety and complications as seen at a liver transplant center. Transplantation 1993 May;55(5):1087-90.

27. McGill DB, Rakela J, Zinsmeister AR, Ott BJ. A 21-year experience with major hemorrhage after percutaneous liver biopsy. Gastroenterology 1990 Nov;99(5):1396-400.

28. Oliva MR, Mortele KJ, Segatto E, Glickman JN, Erturk SM, *et al*. Computed tomography features of nonalcoholic steatohepatitis with histopathologic correlation. J Comput Assist Tomogr. 2006 Jan-Feb;30(1):37-43.

29. Rose C, Vandevenne P, Bourgeois E, Cambier N, Ernst O. Liver iron content assessment by routine and simple magnetic resonance imaging procedure in highly transfused patients. Eur J Haematol. 2006 Aug;77(2):145-9.

30. Alústiza JM, Castiella A, De Juan MD, Emparanza JI, Artetxe J, *et al*. Iron overload in the liver diagnostic and quantification. Eur J Radiol. 2007 Mar;61(3):499-506.

31. Yeh WC, Jeng YM, Li CH, Lee PH, Li PC. Liver steatosis classification using high-frequency ultrasound. Ultrasound Med Biol. 2005 May;31(5):599-605.

32. Oguzkurt L, Yildirim T, Torun D, Tercan F, Kizilkilic O, Niron EA. Hepatic vein Doppler waveform in patients with diffuse fatty infiltration of the liver. Eur J Radiol. 2005 May;54(2):253-7.

33. Sadeeh S, Younossi ZM, Remer EM, et al. The utility of radiological imaging in nonalcoholic fatty liver disease. Gastroenterology 2002;123:745–50.

34. Mottin CC, Moretto M, Padoin AV, Swarowsky AM, Toneto MG, *et al*. The role of ultrasound in the diagnosis of hepatic steatosis in morbidly obese patients. Obes Surg. 2004 May;14(5):635-7.

35. Liang RJ, Wang HH, Lee WJ, Liew PL, Lin JT, Wu MS. Diagnostic value of ultrasonographic examination for nonalcoholic steatohepatitis in morbidly obese patients undergoing laparoscopic bariatric surgery. Obes Surg. 2007 Jan;17(1):45-56.

36. Saadeh S, Younossi ZM, Remer EM, Gramlich T, Ong JP, *et al*. The utility of radiological imaging in nonalcoholic fatty liver disease. Gastroenterology. 2002 Sep;123(3):745-50.

37. Chan DF, Li AM, Chu WC, Chan MH, Wong EM, *et al*. Hepatic steatosis in obese Chinese children. Int J Obes Relat Metab Disord. 2004 Oct;28(10):1257-63.

38. Tominaga K, Kurata JH, Chen YK, Fujimoto E, Miyagawa S, *et al*. Prevalence of fatty liver in Japanese children and relationship to obesity. An epidemiological ultrasonographic survey. Dig Dis Sci. 1995 Sep;40(9):2002-9.

39. Mendler MH, Bouillet P, Le Sidaner A, Lavoine E, Labrousse F, *et al*. Dual-energy CT in the diagnosis and quantification of fatty liver: limited clinical value in comparison to ultrasound scan and single-energy CT, with special reference to iron overload. J Hepatol. 1998 May;28(5):785-94.

40. Kodama Y, Ng CS, Wu TT, Ayers GD, Curley SA, *et al.* Comparison of CT methods for determining the fat content of the liver. AJR Am J Roentgenol. 2007 May;188(5):1307-12.

41. Limanond P, Raman SS, Lassman C, Sayre J, Ghobrial RM, *et al.* Macrovesicular hepatic steatosis in living related liver donors: correlation between CT and histologic findings. Radiology. 2004 Jan;230(1):276-80.

42. Park SH, Kim PN, Kim KW, Lee SW, Yoon SE, *et al.* Macrovesicular hepatic steatosis in living liver donors: use of CT for quantitative and qualitative assessment. Radiology. 2006 Apr;239(1):105-12. Epub 2006 Feb 16.

43. Cho CS, Curran S, Schwartz LH, Kooby DA, Klimstra DS, *et al*. Preoperative radiographic assessment of hepatic steatosis with histologic correlation. J Am Coll Surg. 2008 Mar;206(3):480-8.

44. Duman DG, Celikel C, Tüney D, Imeryüz N, Avsar E, *et al*. Computed tomography in nonalcoholic fatty liver disease: a useful tool for hepatosteatosis assessment? Dig Dis Sci. 2006 Feb;51(2):346-51.

45. Lee JK, Dixon WT, Ling D, Levitt RG, Murphy WA Jr. Fatty infiltration of the liver: demonstration by proton spectroscopic imaging. Preliminary observations. Radiology. 1984 Oct;153(1):195-201.

46. Mitchell DG, Kim I, Chang TS, Vinitski S, Consigny PM, *et al*. Fatty liver. Chemical shift phase-difference and suppression magnetic resonance imaging techniques in animals, phantoms, and humans. Invest Radiol. 1991 Dec;26(12):1041-52.

47. Kim SH, Lee JM, Han JK, Lee JY, Lee KH, *et al*. Hepatic macrosteatosis: predicting appropriateness of liver donation by using MR imaging--correlation with histopathologic findings. Radiology. 2006 Jul;240(1):116-29.

48. Fishbein M, Castro F, Cheruku S, Jain S, Webb B, *et al*. Hepatic MRI for fat quantitation: its relationship to fat morphology, diagnosis, and ultrasound. J Clin Gastroenterol. 2005 Aug;39(7):619-25.

49. Liu CY, McKenzie CA, Yu H, Brittain JH, Reeder SB. Fat quantification with IDEAL gradient echo imaging: correction of bias from T(1) and noise. Magn Reson Med. 2007 Aug;58(2):354-64.

50. Kim SH, Lee JM, Kim JH, Kim KG, Han JK, *et al*. Appropriateness of a donor liver with respect to macrosteatosis: application of artificial neural networks to US images--initial experience. Radiology. 2005 Mar;234(3):793-803.

51. Longo R, Pollesello P, Ricci C, et al. Proton MR spectroscopy in quantitative in vivo determination of fat content in human liver steatosis. J Magn Reson Imaging 1995;5:281–5.